

Unidirectional Extraordinary Sound Transmission with Mode-Selective Resonant Materials

Jie Zhu^{✉,‡}, Xuefeng Zhu,[†] Xiaobo Yin, Yuan Wang, and Xiang Zhang[†]

Nanoscale Science and Engineering Center, University of California, Berkeley, California, USA



(Received 15 January 2020; revised manuscript received 6 March 2020; accepted 23 March 2020; published 17 April 2020)

Unidirectional wave propagation can introduce strong direction-dependent energy responses, and thus, greatly benefits the construction of switching and logic devices. Such an effect has drawn much attention in acoustics, but has not been able to practically address the essential issue of insufficient transmission efficiency in the forward direction. Here, we present a one-way structure that experimentally realizes near-total forward acoustic wave transportation, while still maintaining a broadband high contrast ratio and single-mode property. The experimentally observed rectification is achieved with a comprehensive design of combining acoustic wave intermode transitions, selective-mode filtering, and cavity resonance for strong wave-structure interactions. The demonstrated simplicity and flexibility make this material an appealing integration solution, enabling an alternative control methodology in biomedical ultrasonography, high-performance acoustic sensors, and noise control.

DOI: [10.1103/PhysRevApplied.13.041001](https://doi.org/10.1103/PhysRevApplied.13.041001)

One-way wave propagation has attracted increasing attention from researchers in various fields [1–7], as a special form of energy flow that provides crucial functionality in electronic [8,9], photonic [10–13], mechanical [14], and thermal systems [15–18]. The concepts of time and space reversal symmetry breaking are exploited in designing materials and devices that allow the energy flux to travel in a unidirectional fashion. Switch and rectification devices have revolutionized aspects of modern science and industry. The effects of nonlinearity, structural asymmetry, magnetic field and time-varying to unidirectional transmission of energy have also been extensively studied. The development of an acoustic counterpart is also of crucial importance, where directional sound waves could provide a competing solution for sharpening ultrasound images, enabling novel types of noise control, and acoustic logic switches.

The first one-way control device for acoustic waves proposed by Liang *et al.* [19] breaks the constraints of symmetric transmission by employing phononic crystals and highly nonlinear materials. However, the involved nonlinearity brought out a low transmission rate and nontrivial frequency shift, which is the same as utilizing bifurcation and chaos in a periodic dynamic system [2]. For linear cases, unidirectional acoustic wave propagation with a higher transmission rate is achieved with momentum manipulation [20–23], yet the utilization of diffraction

structures introduces the inevitable wave-vector direction change and phase disturbances. These destructive side effects will most likely cause damaged data or sound signal loss. Active mechanisms utilizing piezoelectricity and time variance have also been successfully demonstrated [24–26]. Although active components can uplift the transmission rate into perfection and even break the reciprocity for complete sound isolation, other crucial issues emerge, for example, a complex system, due to the stringent requirement of a power supply for circuits [24] or motors [25], energy consumption to support strong circuit nonlinearity, signal processing, or air-flow modulation. Recently, right-angle prisms made of zero-index metamaterials were demonstrated to enable unidirectional sound propagation without phase distortion, but suffered from severe loss in space-coiling structures [27]. Non-Hermitian acoustic systems, such as parity-time-symmetric crystals and lossy metasurfaces [28–30], were discovered to produce unidirectional sound diffractions. Acoustic topological insulators also support one-way sound transport on the surface [31–35]. However, these proposals still suffer from the aforementioned problems of nontrivial loss, phase disturbances, complex structures, and so forth.

Here, we show that, by designing a passive unidirectional acoustic resonant material, which takes advantage of acoustic mode conversion, selective mode reflection, and cavity resonance, we are able to experimentally demonstrate not only a broadband high sound-transmission contrast ratio, but, most importantly, near-total transmission and single-mode output in the forward direction. The principle of the proposed acoustic materials is intrinsically distinguished from previous approaches. By accurately

^{*}jie.zhu@polyu.edu.hk

[†]xiang@berkeley.edu

[‡]These authors contributed equally to this work.

tuning semitransparent acoustic mirrors with an intermediate mode converter, all elements resonate concurrently at the operating frequency, driving the forward-direction transmission efficiency into a maximum approaching 100%.

As shown in Fig. 1, the unidirectional acoustic resonant materials consist of two parallel rigid plates with periodically arranged sided gratings and centered rectangular bars. Such a two-dimensional (2D) unidirectional device can be treated as a composite material that consists of three periodic elements, which are highlighted with different colors in Fig. 1(b): the grating structure, element II, which is antisymmetric about the horizontal axis, connects grating element I and center bars of element III at both ends. Inside a uniform waveguide, propagating even-mode and odd-mode acoustic waves exist. When the symmetric scatterers are introduced, these modes will remain decoupled, in terms of topological symmetry, with the formation of band gaps. Due to the different energy distribution nature of even- and odd-mode acoustic waves inside the waveguide, the introduction of sidewall-attached scatterers, such as element I, can effectively block only the odd modes, to form large band gaps. For the structures such as element III, with scatterers in the middle plane, large band gaps for the even modes can be observed. For the antisymmetric configuration of scatterers, the field distribution of

eigenmodes also becomes antisymmetric. Therefore, the antisymmetric field in element II can be regarded as the superposition of even and odd eigenmodes, which indicates strong coupling and conversion between them [36]. At the working frequency, as illustrated in Fig. 1(c), element II converts incident acoustic waves into odd-mode ones due to its intrinsic antisymmetric geometry. Elements I and III behave as semitransparent mode-selective barriers that, respectively, block odd- and even-mode acoustic waves, but allow the passing through of even- and odd-mode components. Together, they form an asymmetric composite material that draws forward-propagating plane waves inside through element I, but rejects the ones coming from the reverse direction when they encounter element III. At the same time, the three elements also independently function as acoustic cavities due to impedance mismatches, mode conversions, and selective rebounds. At a frequency that satisfies all cavity resonance conditions of these cavities, all back-reflecting components can be perfectly cancelled out, as a result of destructive interferences [37,38]. Therefore, the associated forward transmission coefficient has a unity modulus. Our unidirectional materials can be intuitively regarded as providing an additional wave vector, q , to shift the incident even-mode acoustic waves by an additional spatial frequency. The unique thing, as pictured in Fig. 1(d), is that such

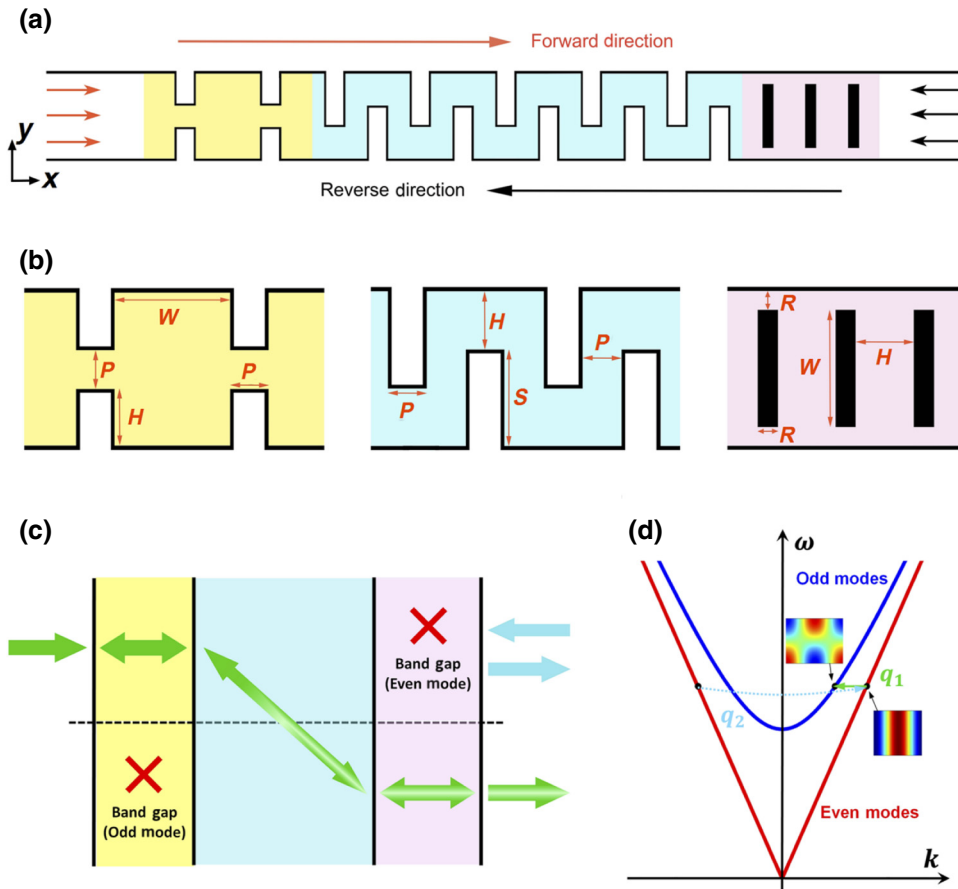


FIG. 1. (a) Waveguide material consisting of elements I (yellow), II (blue), and III (pink). (b) Three elements are designed to have geometry parameters $P = 26.90$ mm, $H = 40.34$ mm, $W = 80.69$ mm, $S = 67.24$ mm, and $R = 13.45$ mm. (c) Unidirectional extraordinary acoustic wave transmission is due to asymmetric wave-manipulation functions provided by three elements. In forward direction, the even-mode incident plane wave (Green arrow) will be totally converted into odd-mode output through mode conversion in element II, selective blocking in elements I and III, and cavity resonances in all elements. Reverse direction incidents will be blocked by element III due to the band gap. (d) Proposed material can be intuitively regarded as providing distinct direction-dependent additional wave vectors: q_1 in forward direction and q_2 in reverse direction.

an additional wave vector is orientation dependent: for forward propagation, $q_1 = k_2 - k_1$, while $q_2 = 2k_1$ when the incident waves travel in the reverse direction. Here, k_1 and k_2 are, respectively, the wave vectors of even- and odd-mode acoustic waves. For any incident even-mode acoustic waves, complete intermode transitions to odd-mode output wave will occur only when the phase-matching condition $k_{\text{output}} = k_1 + q = k_2$ is satisfied. In our case, such a scenario happens only when the acoustic waves travel along the forward direction, where $q = q_1$. For backward propagation, the momentum, q_2 , will make $k_{\text{output}} = -k_1 + q_2 = k_1$, which indicates total reflection of the incident acoustic waves. It is worth mentioning that

the one-way tunneling mode conversion for high-ordered even and odd modes may be observed by following our proposed design rule. However, the high-ordered modes often overlap with low-ordered modes of the same modal symmetry in the band structure. Therefore, designing a simple structure for selective high-ordered mode filtering and intermode transitions is challenging.

To substantiate the overall performance, full-wave 2D finite element method (FEM) simulation is implemented. From the simulation results presented in Figs. 2 and 3, it is clearly evident that the acoustic waves traveling in opposite directions have dramatically different transmission properties. In the forward direction, the transmission

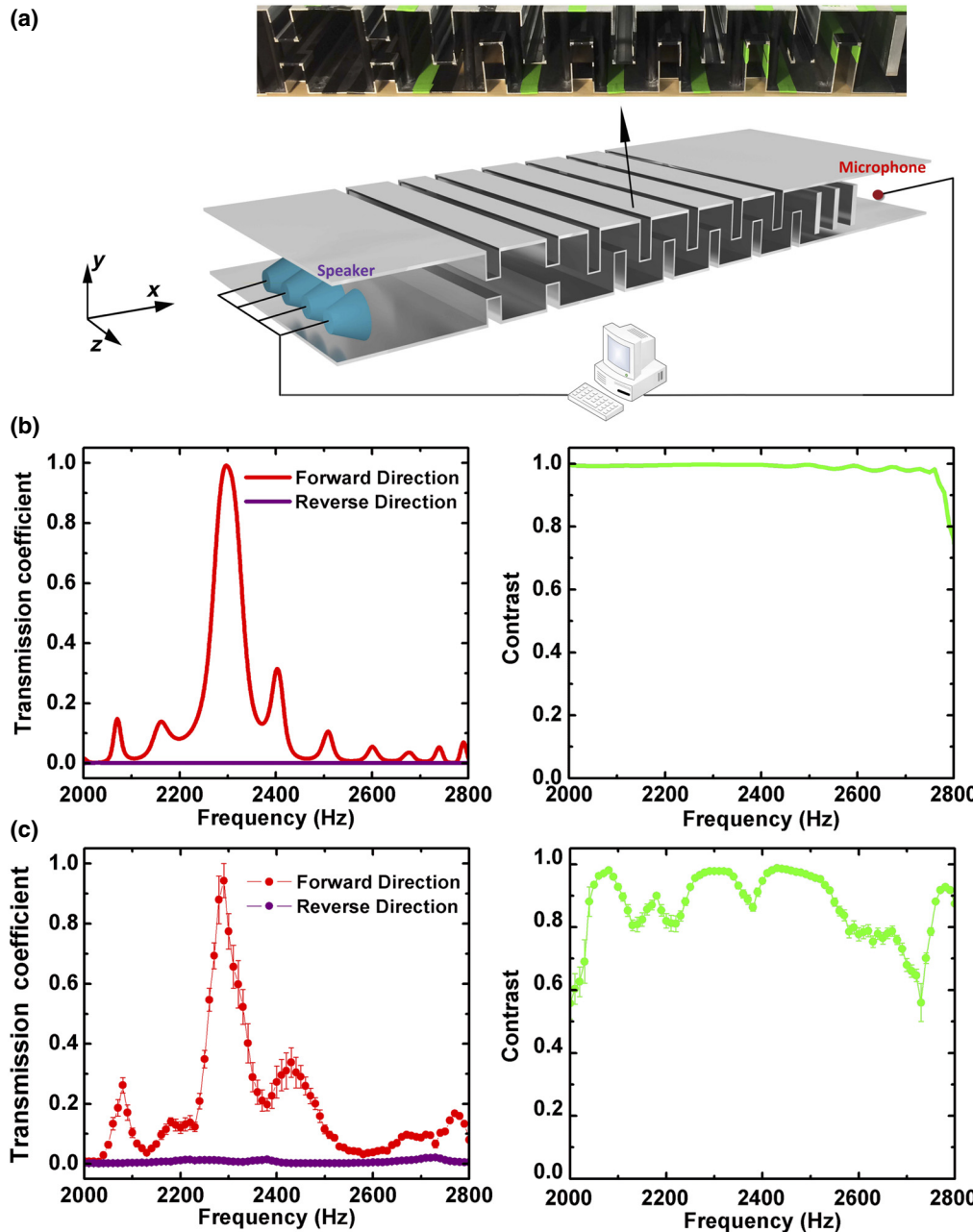


FIG. 2. (a) Schematic of the experiment setup and fabricated sample. (b) Simulated transmission contrast (green line) and acoustic energy transmission coefficients in forward (red line) and reverse directions (purple line). Transmission peaks can be observed in forward direction between 2000 and 2800 Hz, with the major peak located at 2290 Hz. (c) Measured forward and reverse direction transmission coefficients and contrast. Major peak in forward direction is at 2280 Hz. Signals measured in reverse direction are mostly background noise, which also cause the contrast change in experimental results. Error bars represent s.d. among five repeat measurements.

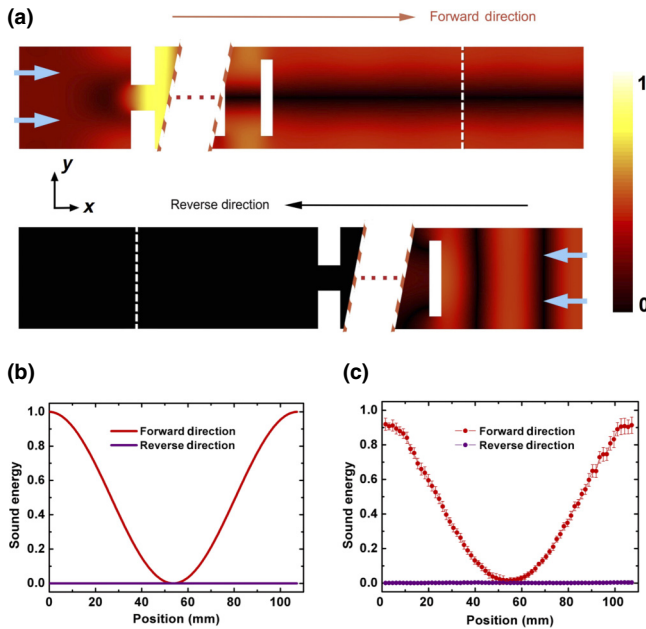


FIG. 3. (a) Simulated output sound field maps for forward and backward propagations. Incident even-mode waves tunnel through the materials without reflections and are converted into odd modes, while no transmission is observed for the same incident even-mode waves coming from the reverse direction. Waveguide material section is represented by the dotted line to save space. (b) Normalized simulation and (c) experimental measurements of output sound energy field along the marked lines in forward and backward directions. Operating frequency for simulation is 2290 Hz, while experimental data are acquired at 2280 Hz.

coefficient, which can be defined as the ratio between transmitted sound energy with and without the proposed structure, shows spectral variation within the band of interest. It reaches near 100% around 2290 Hz, at which frequency all elements work at the cavity resonance modes, closely resembling the function of a double-barrier resonant tunneling diode [39,40]. Such a transmission ratio in the reverse direction, however, always stays close to zero within the same frequency range because of the band-gap effect. We further demonstrate the unidirectional performance by calculating the contrast, which can be defined as [22]

$$C = \frac{T_{FD} - T_{RD}}{T_{FD} + T_{RD}}, \quad (1)$$

where T_{FD} and T_{RD} are, respectively, transmission coefficients in forward and reverse directions. As shown in Figs. 2(b) and 2(c), the unidirectional transmission effect is strongly witnessed by the value of C remaining near one.

We conduct the experiments in air at room temperature with a setup schematically sketched in Fig. 2(a). The structure is assembled from aluminum alloy materials. Such alloy metal can be treated as a rigid materials, as in our

FEM simulation. To diminish reflection at the waveguide output openings, we not only add sound-absorbing foam, but also attach a curved structure, so the impedance mismatch can be offset. Along the x direction, we include all experimental data measured in an area 2 times the wavelength, when we further calculate the transmission coefficient in Fig. 2(b), and test the material's performance within the frequency of interest, which is from 2000 to 2800 Hz with a step of 10 Hz based on the prediction of the FEM simulation. The spectral evolution of the acoustic wave transmission coefficient and contrast ratio is presented in Fig. 2(c). Although there is a 10 Hz frequency shift for the location of the peak between experimental results (2280 Hz) and simulation predictions (2290 Hz), the experimental results in both forward and reverse directions match the simulation outputs very well. The measured forward-direction transmission coefficient varies with frequency, peaking at 2280 Hz, with 93% of the total energy transmitted through compared with the case of uniform waveguide. It is significantly higher than that of previous typical passive unidirectional acoustic transmission solutions [2,19–22]. In the reverse direction, although still at a very low level, the experimentally acquired transmissions are higher than that suggested by the simulation due to ambient noise, which also leads to less-perfect contrasts compared with those of simulation outputs. Nevertheless, the material possesses a satisfactory high-contrast value along a broad bandwidth.

In Fig. 3, we further present the sound amplitude field maps for forward and backward propagations at the tunneling frequency. The mode transition of the output propagating wave along the forward direction is clearly observed in both X - Y and Y - Z [41] planes with the presence of an odd-mode-type silent zone between the two strong marginal acoustic fields. The fact that, while the transmitted acoustic signal in the forward direction is strong, the one in the reverse direction is dramatically weaker (more than two orders of magnitude) and barely measurable evidently demonstrate the unidirectional acoustic wave transmission.

The effect of viscothermal losses are numerically simulated [41]. The module of narrow-region acoustics is imposed on all subwavelength slits. At the resonance frequency, peak values of normalized output sound energy fields are very close to each other, for respective cases with and without considering viscothermal losses.

The near-perfect acoustic tunneling phenomenon in the forward direction, by design, is the product of simultaneous excitation of preferred mode resonance within all three founding elements shown in Fig. 1(b). Since these three elements are finite-sized periodic structures, we calculate their respective band structures and transmission coefficients through the supercell approximation technique [41] and FEM. The results are plotted as separate curves in

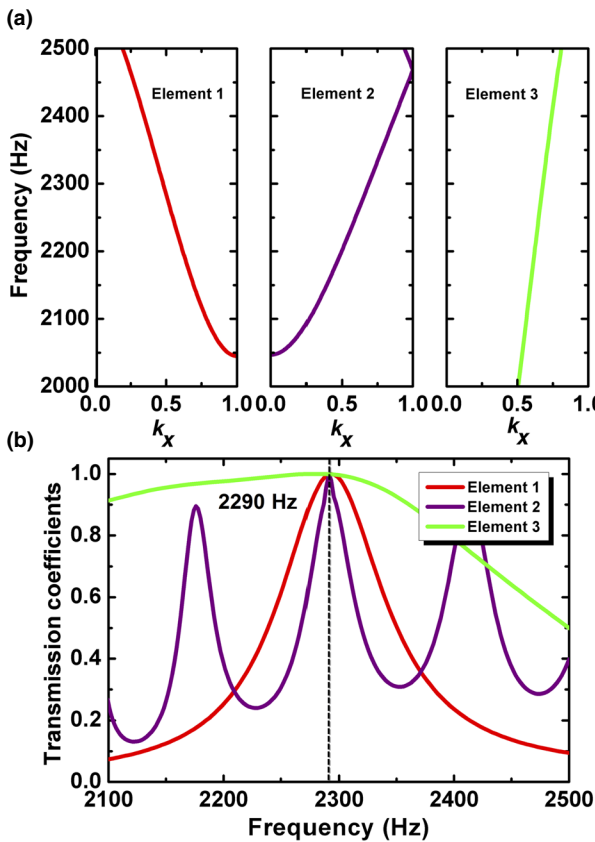


FIG. 4. (a) Calculated band structures of pure even mode (red line) within element I, hybrid mode (purple line) within element II, and pure odd mode (green line) within element III. (b) To design a unidirectional acoustic resonance material, as presented, all three elements have to be tuned to have cavity resonance peak at 2290 Hz, as marked by the black line, so that near-total transmission through the whole waveguide materials in the forward direction can be realized.

Fig. 4(a), demonstrating the transmission performance of each element within the passing band of preferred modes. Within the frequency range of 2100–2500 Hz, elements I and III, respectively, allow only the existence of pure even-mode and odd-mode acoustic waves, while more-complex hybrid modes dominate inside element II. Each element can be regarded as an acoustic cavity. It is important to note that, to realize unidirectional perfect acoustic wave transmission, all three elements must be accurately tuned to have one of their cavity resonant modes located exactly at the operating frequency, for example, 2290 Hz, in our case, as marked with black line in Fig. 4(b). Therefore, the transmission can reach 100%, when all elements are simultaneously reaching the resonant states. This phenomenon is closely related to a singularity point of the scattering matrix [42], where the dynamic change of the hidden topology can be observed by the occurrence of an abrupt phase transition of π for the reflected waves [41]. It needs to be pointed out that there is a lower limit for the unit-cell

number of three elements. Numerical simulations show that, when the unit-cell numbers in three elements are each reduced by one. Although a stark transmission contrast still exists, a near-unitary transmission cannot be reached in the forward direction, as the resonance condition is breaking [41].

Here, we propose an approach to design unidirectional acoustic resonant materials that combine acoustic wave mode conversion and filtering with cavity resonance tuning to accomplish one-way extraordinary sound transmission, which is experimentally demonstrated. Other than our design, it can also be constructed from other symmetric and antisymmetric waveguide structures. This type of material is not only suitable for switch and rectification function, but also extremely valuable for signal-sensitive acoustic applications, such as communications and sensing of weak signals. Further trimming the material's geometry or increasing the number of periodic structures will expand the near-total transmission spectrally to meet the demand of broadband scenarios. Our approach may also be implemented in elastic or optic systems due to the similar governing wave equation.

ACKNOWLEDGMENTS

The work is supported by the Ernest S. Kuh Endowed Chair Professorship.

- [1] L. A. Coldren, S. W. Corzine, and M. L. Mashanovitch, *Diode Lasers and Photonic Integrated Circuits* (John Wiley & Sons, Inc., Hoboken, New Jersey, USA, 2012).
- [2] N. Boehler, G. Theocharis, and C. Daraio, Bifurcation-based acoustic switching and rectification, *Nature Mater.* **10**, 665 (2011).
- [3] H. Jia, M. Z. Ke, C. H. Li, C. Y. Qiu, and Z. Y. Liu, Unidirectional transmission of acoustic waves based on asymmetric excitation of Lamb waves, *Appl. Phys. Lett.* **102**, 153508 (2013).
- [4] R. Krishnan, S. Shirota, Y. Tanaka, and N. Nishiguchi, High-efficient acoustic wave rectifier, *Solid State Commun.* **144**, 194 (2007).
- [5] S. Lepri and G. Casati, Asymmetric Wave Propagation in Nonlinear Systems, *Phys. Rev. Lett.* **106**, 164101 (2011).
- [6] B. Liang, B. Yuan, and J. C. Cheng, Acoustic Diode: Rectification of Acoustic Energy Flux in One-Dimensional Systems, *Phys. Rev. Lett.* **103**, 104301 (2009).
- [7] J. E. Villegas, S. Savel'ev, F. Nori, E. M. Gonzalez, J. V. Anguita, R. Garcia, and J. L. Vicent, A superconducting reversible rectifier that controls the motion of magnetic flux quanta, *Science* **302**, 1188 (2003).
- [8] P. Horowitz and H. Winfield, *The art of Electronics* (Cambridge University Press, Cambridge, UK, 1989).
- [9] S. Steudel, K. Myny, V. Arkhipov, C. Deibel, S. De Vusser, J. Genoe, and P. Heremans, 50MHz rectifier based on an organic diode, *Nature Mater.* **4**, 597 (2005).

- [10] F. D. M. Haldane and S. Raghu, Possible Realization of Directional Optical Waveguides in Photonic Crystals with Broken Time-Reversal Symmetry, *Phys. Rev. Lett.* **100**, 013904 (2008).
- [11] J. Hwang, M. H. Song, B. Park, S. Nishimura, T. Toyooka, J. W. Wu, Y. Takanishi, K. Ishikawa, and H. Takezoe, Electro-tunable optical diode based on photonic bandgap liquid-crystal heterojunctions, *Nature Mater.* **4**, 383 (2005).
- [12] Z. Wang, Y. D. Chong, J. D. Joannopoulos, and M. Soljacic, Reflection-Free One-Way Edge Modes in a Gyromagnetic Photonic Crystal, *Phys. Rev. Lett.* **100**, 013905 (2008).
- [13] Z. F. Yu and S. H. Fan, Complete optical isolation created by indirect interband photonic transitions, *Nature Photon.* **3**, 91 (2009).
- [14] V. F. Nesterenko, C. Daraio, E. B. Herbold, and S. Jin, Anomalous Wave Reflection at the Interface of Two Strongly Nonlinear Granular Media, *Phys. Rev. Lett.* **95**, 158702 (2005).
- [15] C. W. Chang, D. Okawa, A. Majumdar, and A. Zettl, Solid-State thermal rectifier, *Science* **314**, 1121 (2006).
- [16] B. W. Li, J. H. Lan, and L. Wang, Interface Thermal Resistance Between Dissimilar Anharmonic Lattices, *Phys. Rev. Lett.* **95**, 104302 (2005).
- [17] B. W. Li, L. Wang, and G. Casati, Thermal Diode: Rectification of Heat Flux, *Phys. Rev. Lett.* **93**, 184301 (2004).
- [18] L. Wang and B. Li, Thermal Logic Gates: Computation with Phonons, *Phys. Rev. Lett.* **99**, 177208 (2007).
- [19] B. Liang, X. S. Guo, J. Tu, D. Zhang, and J. C. Cheng, An acoustic rectifier, *Nature Mater.* **9**, 989 (2010).
- [20] X. F. Zhu, X. Y. Zou, B. Liang, and J. C. Cheng, One-way mode transmission in one-dimensional phononic crystal plates, *J. Appl. Phys.* **108**, 124909 (2010).
- [21] Z. J. He, S. S. Peng, Y. T. Ye, Z. W. Dai, C. Y. Qiu, M. Z. Ke, and Z. Y. Liu, Asymmetric acoustic grating, *Appl. Phys. Lett.* **98**, 083505 (2011).
- [22] X. F. Li, X. Ni, L. A. Feng, M. H. Lu, C. He, and Y. F. Chen, Tunable Unidirectional Sound Propagation Through a Sonic-Crystal-Based Acoustic Diode, *Phys. Rev. Lett.* **106**, 084301 (2011).
- [23] S. J. Xu, C. Y. Qiu, and Z. Y. Liu, Acoustic transmission through asymmetric grating structures made of cylinders, *J. Appl. Phys.* **111**, 094505 (2012).
- [24] B. I. Popa and S. A. Cummer, Non-reciprocal and highly nonlinear active acoustic metamaterials, *Nat. Commun.* **5**, 3398 (2014).
- [25] R. Fleury, D. L. Sounas, C. F. Sieck, M. R. Haberman, and A. Alu, Sound isolation and giant linear nonreciprocity in a compact acoustic circulator, *Science* **343**, 516 (2014).
- [26] Y. X. Shen, Y. G. Peng, D. G. Zhao, X. C. Chen, J. Zhu, and X. F. Zhu, One-Way Localized Adiabatic Passage in an Acoustic System, *Phys. Rev. Lett.* **122**, 094501 (2019).
- [27] Y. Li, B. Liang, Z. M. Gu, X. Y. Zou, and J. C. Cheng, Unidirectional acoustic transmission through a prism with near-zero refractive index, *Appl. Phys. Lett.* **103**, 053505 (2013).
- [28] X. F. Zhu, H. Ramezani, C. Z. Shi, J. Zhu, and X. Zhang, PT-Symmetric Acoustics, *Phys. Rev. X* **4**, 031042 (2014).
- [29] T. Liu, X. F. Zhu, F. Chen, S. J. Liang, and J. Zhu, Unidirectional Wave Vector Manipulation in Two-Dimensional Space with an All Passive Acoustic Parity-Time-Symmetric Metamaterials Crystal, *Phys. Rev. Lett.* **120**, 124502 (2018).
- [30] Y. Li, C. Shen, Y. Xie, J. Li, W. Wang, S. A. Cummer, and Y. Jing, Tunable Asymmetric Transmission via Lossy Acoustic Metasurfaces, *Phys. Rev. Lett.* **119**, 035501 (2017).
- [31] Y. G. Peng, C. Z. Qin, D. G. Zhao, Y. X. Shen, X. Y. Xu, M. Bao, H. Jia, and X. F. Zhu, Experimental demonstration of anomalous Floquet topological insulator for sound, *Nat. Commun.* **7**, 13368 (2016).
- [32] C. He, X. Ni, H. Ge, X. C. Sun, Y. B. Chen, M. H. Lu, X. P. Liu, and Y. F. Chen, Acoustic topological insulator and robust one-way sound transport, *Nat. Phys.* **12**, 1124 (2016).
- [33] J. Lu, C. Qiu, L. Ye, X. Fan, M. Ke, F. Zhang, and Z. Liu, Observation of topological valley transport of sound in sonic crystals, *Nat. Phys.* **13**, 369 (2017).
- [34] Y. J. Ding, Y. G. Peng, Y. F. Zhu, X. D. Fan, J. Yang, B. Liang, X. F. Zhu, X. G. Wan, and J. C. Cheng, Experimental Demonstration of Acoustic Chern Insulators, *Phys. Rev. Lett.* **122**, 014302 (2019).
- [35] Y. G. Peng, Y. Li, Y. X. Shen, Z. G. Geng, J. Zhu, C. W. Qiu, and X. F. Zhu, Chirality-assisted three-dimensional acoustic floquet lattices, *Phys. Rev. Res.* **1**, 033149 (2019).
- [36] Z. L. Hou and B. M. Assouar, Opening a band gap in the free phononic crystal thin plate with or without a mirror plane, *J. Phys. D: Appl. Phys.* **41**, 21 (2008).
- [37] M. H. Lu, X. K. Liu, L. Feng, J. Li, C. P. Huang, and Y. F. Chen, Extraordinary Acoustic Transmission Through a 1D Grating with Very Narrow Apertures, *Phys. Rev. Lett.* **99**, 174301 (2007).
- [38] Y. Zhou, M. H. Lu, L. Feng, X. Ni, Y. F. Chen, Y. Y. Zhu, S. N. Zhu, and N. B. Ming, Acoustic Surface Evanescent Wave and its Dominant Contribution to Extraordinary Acoustic Transmission and Collimation of Sound, *Phys. Rev. Lett.* **104**, 164301 (2010).
- [39] H. S. Nguyen, D. Vishnevsky, C. Sturm, D. Tanese, D. Solnyshkov, E. Galopin, A. Lemaitre, I. Sagnes, A. Amo, G. Malpuech, and J. Bloch, Realization of a Double-Barrier Resonant Tunneling Diode for Cavity Polaritons, *Phys. Rev. Lett.* **110**, 236601 (2013).
- [40] B. David, *Quantum Theory* (Prentice-Hall, New York, 1951).
- [41] See the Supplemental Material at <http://link.aps.org/supplemental/10.1103/PhysRevApplied.13.041001> for discussions of the scattering matrix, the viscothermal effects, and the supercell plane-wave expansion method.
- [42] V. Liu, D. A. Miller, and S. Fan, Ultra-compact photonic crystal waveguide spatial mode converter and its connection to the optical diode effect, *Opt. Express* **20**, 28388 (2012).